ELSEVIER

Journal of Nuclear Materials 264 (1999) 257–262

journal of nuclear materials

Fractographic observations of cleavage fracture initiation in a bainitic A508 steel

M. Mäntylä [a,*], A. Rossoll [a], I. Nedbal [b], C. Prioul [a], B. Marini [c]

[a] *Ecole Centrale de Paris, Laboratoire MSS-MAT, CNRS U.R.A. No 850, F-92295 Châtenay-Malabry cedex, France*
[b] *Czech Technical University in Prague, FJFI, Department of Materials, CZ-12000 Prague 2, Czech Republic*
[c] *CEA Saclay, CEREM, SRMA, F-91191 Gif-sur-Yvette cedex, France*

Received 19 May 1998; accepted 17 August 1998

Abstract

Cleavage initiation in CVN (Charpy V-notch) and CT (compact tension) specimens made of a bainitic pressure vessel steel was investigated, in the ductile-to-brittle transition region. The fracture surfaces were examined with a scanning electron microscope (SEM), in order to measure the coordinates of the cleavage initiation sites, and to identify the fractographic and/or microstructural features suspected to have triggered cleavage. Cleavage initiation was found to be promoted by the same microstructural features for both CVN and CT specimens. However, the types of cleavage initiation sites differ over the range of temperature investigated. At low temperatures, small spherical and large elongated inclusions are equally important for cleavage initiation. As the temperature increases, the role of the large MnS inclusions also increases. In 80% of the specimens tested, over the temperature range investigated, manganese sulfides play a major role in cleavage initiation.

1. Introduction

It is commonly assumed that cleavage fracture of ferritic steels on the lower shelf can be induced by some dislocation pile-up mechanism [1], and/or by carbide cracking [2] (see also a review by Hahn [3]). Consequently, for mild steels, grain and/or carbide size have been suggested as the microstructural features controlling cleavage fracture [4]. In the case of more complex microstructures, such as bainitic steels, it is more difficult to define a characteristic microstructural unit playing a role comparable to that of grain size in mild steels: propositions include the lath width [5], the packet or covariant packet size [5,6], and the 'effective' grain size based on the size of the cleavage facets [7]. The carbide diameter has also been invoked as a major factor controlling cleavage fracture in bainite [8].

Many more references than those cited above confirm that cleavage in steel can be initiated by these mechanisms (i.e. dislocation pile-up or carbide cracking). However, only little evidence has been found of the possible role on cleavage fracture of larger *non-metallic inclusions*, e.g. manganese sulfides, whereas their role in ductile fracture is well documented. Tweed and Knott [9,10] seem to be the first ones to report MnS inclusion induced cleavage, in a C–Mn weld metal. Subsequently, further confirmation of possible inclusion-induced cleavage fracture has been found, again for C–Mn weld metal [11], for bainitic A508 or A533 pressure vessel steel [12–18], and for a resulphurized mild steel [19].

Recently, Renevey [20] reported mainly inclusion-induced cleavage initiation in a A508 steel for notched tensile specimens tested at a temperature corresponding to the lower shelf of fracture toughness. Image analysis on polished surfaces yielded a mean inclusion volume fraction of $f_v = 9.4 \times 10^{-4}$ (compared to $f_v = 3.9 \times 10^{-4}$ applying Franklin's formula on manganese sulfides only, or $f_v = 5.7 \times 10^{-4}$ considering oxides also). The mean dimension of inclusions was determined to be 10 ± 2 μm (slightly ellipsoidal). However, fractographic

* Corresponding author. Present address: Tampere University of Technology, Institute of Materials Science, P.O. Box 589, 33101 Tampere, Finland. Tel.: +358-3 365 2294; fax: +358-3 365 2330; e-mail: mmantyla@cc.tut.fi

0022-3115/99/$ – see front matter
PII: S0022-3115(98)00496-6

Table 1
Chemical composition of the material (in weight percent)

C	S	P	Si	Mn	Ni	Cr	Mo	V	Cu	Co	Al	N	O (ppm)	Sn (ppm)	As (ppm)
0.159	0.008	0.005	0.24	1.37	0.70	0.17	0.50	<0.01	0.06	<0.01	0.24	0.007	35–36	50	160

observations indicated a stringer-like shape of the large inclusions (length in the order of 100 μm).

The purpose of our contribution is to present observations on the nature of cleavage initiation sites in the same material, but for CVN (Charpy V-notch) and CT (compact tension) specimens. The large number of specimens employed allowed us to conduct a statistical evaluation. This study is the first step towards micromechanical modelling of cleavage fracture on the lower shelf of the ductile-to-brittle transition.

2. Material and methods

The material examined is a tempered bainitic pressure vessel steel (similar to A508 Cl.3). The chemical composition is given in Table 1. The heat treatment includes two austenitizings followed by water quenching and tempering, and a final stress relief treatment. The final austenite grain size is about 25 μm. Two specimen geometries were studied: standard Charpy V-notch and 25 mm (1T) CT specimens. All specimens were machined in the T–S (long transverse–short transverse) orientation.

Fig. 1 presents the CVN data obtained. All the fracture surfaces were examined with a Philips XL30 scanning electron microscope. An EDAX DX-4 (energy dispersive X-ray analysis) device was employed for analysing the chemical composition of inclusions. The number of specimens examined at each temperature is presented in Table 2.

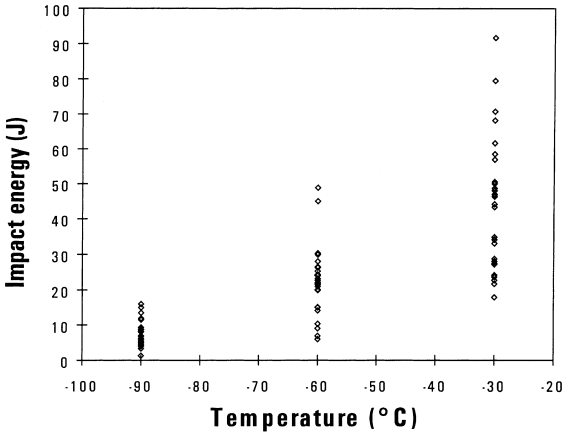

Fig. 1. CVN impact energies obtained at the three levels of test temperature where the fractographic observations have been conducted. The upper shelf energy of the material is in the order of 200 J (at $T = 40$°C).

The scanning electron microscope was used to measure the coordinates of the cleavage initiation sites on the fracture surface and to identify some distinct fractographic and/or microstructural features suspected to have triggered, or at least promoted, cleavage. First, the macroscopic area where cleavage had initiated was located macroscopically, using a similar method as employed in [12,15–18], i.e., tracing back the radial pattern emanating from the crack initiation region (see Fig. 2a). Then higher magnifications were used to follow the fan of ridges, leading to the microscopic cleavage initiation site (see Fig. 2b). However, it shall be emphasized that this fractographic work is of considerable difficulty, especially in the case of specimens fractured at low temperature (with a low toughness value) that exhibit a very flat fracture surface and only rarely macroscopic cleavage fans.

In that case, frequently multiple cleavage initiation sites were found. We address as 'principal' site the location that seems to have triggered global failure of the specimen. It can be speculated whether 'secondary' sites were activated *prior* to the principal site, and induced cracks that were arrested prior to macroscopic failure of the specimen, or as sites that were triggered by the advance of the main crack, thus *after* the activation of the main site. The latter interpretation seems more plausible. The principal sites were identified by a method similar to the one described by Miglin et al. [15], i.e. considering the importance of pronounced ridge fans.

The fractographic identification of the cleavage initiation sites was followed by their localisation on the fracture surface. The principle of the coordinate measurement was the same for both types of specimen. Fig. 3 depicts the nomenclature employed for Charpy specimens. Coordinate x is the distance from the edge of the specimen to the cleavage initiation site. Coordinate y_1 is the distance from the notch to the initiation site, and coordinate y_2 the distance from the ductile crack front to the site. The x-coordinate is measured in a similar manner in CT specimens, but y-coordinates were

Table 2
Number of specimens examined

Specimen type	$T = -90$°C	$T = -60$°C	$T = -30$°C
CVN	29	27	28
CT	25	9	4

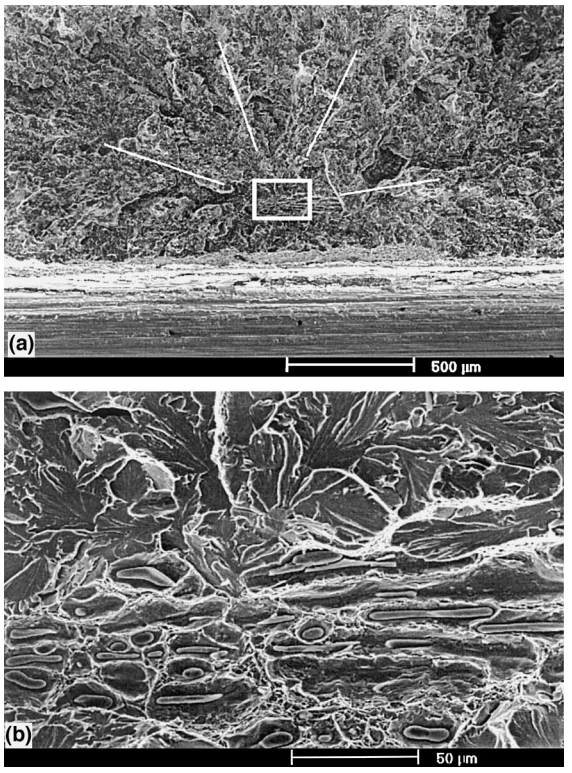

Fig. 2. Principle used for tracing back the cleavage initiation site: (a) Low magnification showing the fan of ridges starting from the central area in the photograph; (b) High magnification showing a cluster of MnS inclusions that has apparently promoted cleavage initiation.

defined slightly differently: since CT specimens contain a fatigue pre-crack and showed no ductile crack growth, a y_3-coordinate was introduced. It represents the distance from the fatigue pre-crack to the cleavage initiation site.

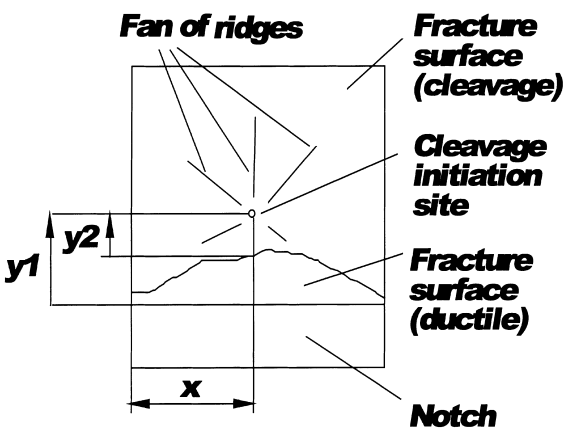

Fig. 3. Principle of the coordinate measurement in Charpy specimens.

3. Results and discussion

Occurrence of multiple initiation sites. For both Charpy and CT specimens, the number of cleavage initiation sites decreased with increasing temperature. An average number of 1.07 sites per KCV specimen were identified at the highest temperature investigated (−30°C), and an average of 2.5 at the lowest temperature (−90°C). Sites were found to be more numerous in CT specimens, which seems also to be due to the larger specimen width. The results presented in the following concern only the principal sites.

Types of cleavage initiation sites. Different types of cleavage initiation sites could be distinguished. However, the principal categories were the same for both specimen geometries. They were classified as follows:

1. Small, approximately spherical inclusion (diameter approximately 2–3 μm), often composed of MnS and/or oxide (see Fig. 4),
2. large, elongated inclusion mainly composed of MnS, in form of a stringer (length in the order of 100 μm), or cluster of large inclusions (see Fig. 2b),
3. any other particular feature that was encountered in the cleavage initiation area, and that possibly played a role in cleavage initiation: grain boundary, cluster of large cleavage facets (indicating abnormally large grains), ductile/cleavage interface (identified only in Charpy specimens), carbide inside a grain (identified only in CT specimens), stretch zone (only in CT specimens). However, these features could not be associated with cleavage initiation with certainty.

The most frequently detected initiation sites were small spherical or large elongated inclusions (manganese sulfides). The category of small inclusions includes also small MnS inclusions, since the classification is based on the size and the shape of the inclusion. When a large

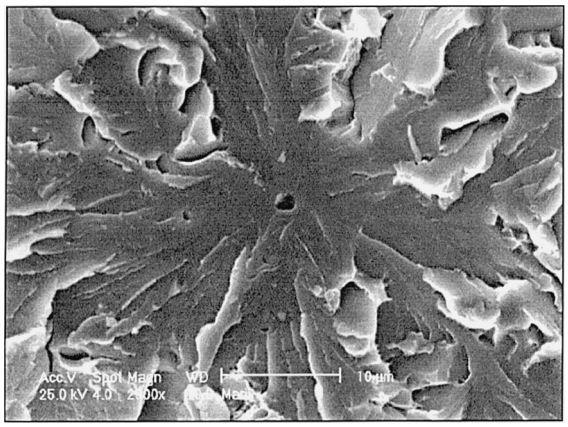

Fig. 4. Cavity in the centre of a cleavage facet. The small inclusion appearing to have initiated cleavage fracture has debonded.

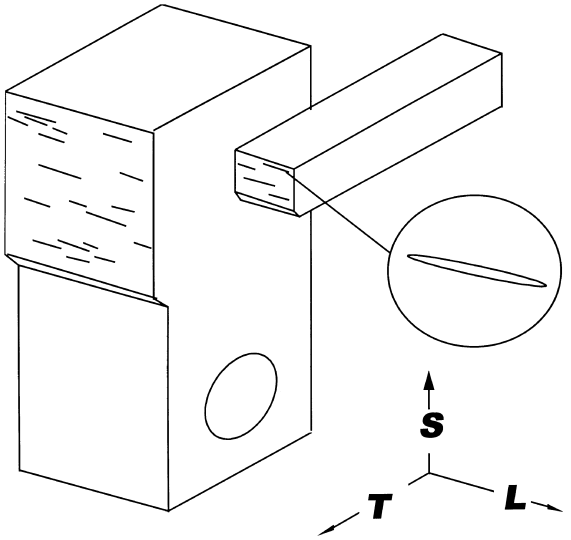

Fig. 5. Orientation of elongated inclusions in relation to the specimen orientation.

MnS inclusion or a cluster of MnS inclusions had initiated cleavage, the fan of ridges could usually be traced back to several locations around the inclusion or the cluster. In the case of parallel occurrence of both large MnS particles and another feature (e.g. small inclusion) in its vicinity, the site was classified as 'large inclusion', although the actual triggering point might have been the smaller feature. This 'overrunning' of any other feature by large inclusions seems justified, as these large heterogeneities increase the stresses in their vicinity, and may activate sites that would not be potent enough to act alone. This influence of large elongated inclusions on cleavage initiation has already been suggested by Baker et al. [19]. Fig. 2(b) gives an example where cleavage has initiated next to a large cluster of MnS stringers. This is why the initiation site is classified as 'large inclusion', even though the actual initiation site might have been another feature, e.g. a small inclusion or a grain boundary.

The orientation of elongated inclusions, due to the forging process, is schematically depicted in Fig. 5. It is well known that the interfacial strength of MnS inclusions is rather low, resulting in early debonding during the loading process [21,22]. Eventually, debonding already occurs prior to loading due to thermal contraction, since the thermal expansion coefficient of manganese sulfide is higher than that of the matrix [23]. For the specimen orientation examined (T–S), the occurrence of a cluster of MnS stringers will thus result in a plate-like defect, which has also been observed in notched tensile specimens examined by Renevey [20], who studied the same material. The same effect is diagnosed in the S–T orientation [14]. It is evident that such a defect will promote brittle failure.

Temperature has a pronounced effect on the type of active cleavage initiation site (see the results for Charpy specimens in Table 3). At −90°C small and large inclusions were found equally responsible for cleavage initiation. At higher temperatures, the contribution of large inclusions (MnS) increased. At −30°C the small inclusions alone were not able to initiate cleavage. At this temperature, in almost all cases cleavage fracture was initiated due to the presence of the large MnS inclusions. No correlation could be found between the type of initiation site and the absorbed energy in Charpy specimens, or the fracture toughness in CT specimens respectively.

Coordinates of the cleavage initiation sites. Temperature affects also the coordinates of the cleavage initiation sites. Fig. 6 shows the influence of temperature on the x-coordinates of the principal sites in Charpy specimens. At −90°C the x-coordinates (i.e. the distance between the edge and the site) of the sites are located homogeneously along the specimen width (except close to the surface). At higher temperatures, the sites tend to situate more and more in the centre. The same behaviour is also detected in CT specimens. This fractographic finding indicates that constraint plays a more important role on cleavage initiation at higher temperatures.

Coordinates x and y are not correlated. No correlation can also be found between the x-coordinate and the absorbed energy (Charpy specimens) or the fracture toughness (CT specimens).

In Charpy specimens tested at temperatures −90°C and −60°C no correlation is found between coordinate y_1 (i.e. the distance from the notch root to the site) and the absorbed energy. At −30°C the absorbed energy increased with coordinate y_1, as to be seen in Fig. 7. This is due to the important amount of ductile tearing preceding cleavage fracture observed at this temperature. Obviously ductile crack advance consumes significantly

Table 3
Effect of temperature on the type of cleavage initiation site in Charpy specimens (principal sites only)

Type	Number of occurences		
	$T=-90$°C	$T=-60$°C	$T=-30$°C
Small spherical inclusion	9 (31%)	9 (33%)	0
Large elongated inclusion (MnS)	14 (48%)	17 (63%)	27 (96%)
Other	6 (21%)	1 (4%)	1 (4%)

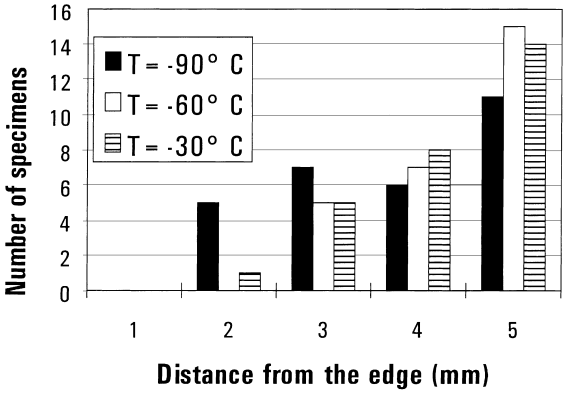

Fig. 6. Charpy specimens – influence of the test temperature on the x-coordinates of the principal initiation sites.

more energy than cleavage, so that a strong correlation can be found between the size of the ductile crack initiation zone and the CVN value [24]. This is analogous to the behaviour commonly observed in fracture toughness testing, where increasing ductile crack advance gives rise to an increasing resistance to fracture (in terms of the J–Δa fracture resistance curve).

Since the yield stress of the material and hence the general level of stresses is lower at higher temperature, only a few (the most critical) potential cleavage triggering sites remain active. The population of possible sites is thus reduced at a higher temperature. This means that, statistically, a larger volume of material has to be sampled by the advancing high stress zone in front of the crack, in order to encounter a weak spot capable of triggering cleavage. Ductile crack advance prior to cleavage is thus more important at a higher temperature.

The distance between the ductile crack tip and the site (coordinate y_2) varies between 0.1–0.5 mm but it is temperature independent in the temperature range tested. In CT specimens the lower bound value of fracture toughness increased as the distance from the fatigue pre-crack to the principal site increased (Fig. 8). The same behaviour is observed at temperatures −60°C and −30°C, even though the number of observations was smaller.

The lateral location (x-coordinates) of the cleavage initiation site depends on their nature. It is found that small inclusions can initiate cleavage fracture only in the centre of the specimen where stresses and constraint are higher. This explains why this type of site is not observed anymore at higher temperatures, due to the lower stresses present (see Table 3). For other types of cleavage initiation sites there was no correlation between the type of initiation site and its x-coordinate. No correlation could be established between the type of initiation site and coordinates y_1, y_2 and y_3.

4. Conclusions

Cleavage initiation was found to be promoted by the same microstructural features for both CVN and CT specimens. However, the types of cleavage initiation sites that were encountered differ over the range of temperature investigated. At low temperatures, small spherical and large elongated inclusions were equally important for the cleavage initiation. As the temperature increases, the role of the large MnS inclusions also increases, and at −30°C the small inclusions are not able to initiate cleavage. In 80% of the specimens tested, over the temperature range investigated, manganese sulfides play a major role in cleavage initiation.

Temperature appears to affect also the coordinates of the cleavage initiation sites. At low temperatures, the principal sites are located rather homogeneously along the specimen width. For higher temperatures, the sites tend to shift closer to the centre of the specimen, and to be less numerous. In CT specimens, the lower bound

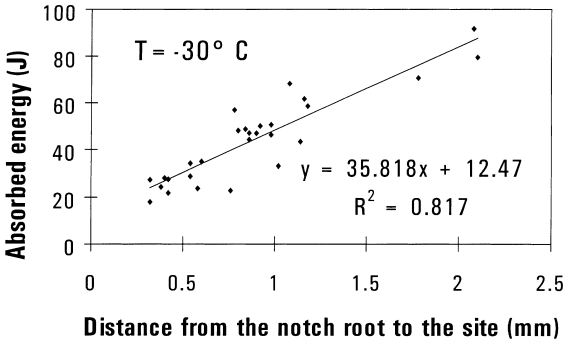

Fig. 7. Charpy specimens tested at $T = -30$°C – relation between the distance from the notch to the principal initiation site (coordinate y_1) and the absorbed energy.

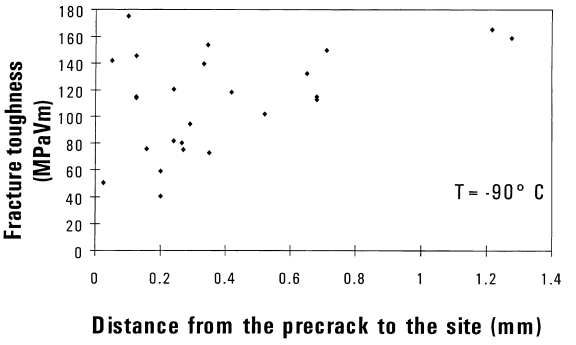

Fig. 8. CT specimens tested at $T = -90$°C – relation between the distance from the fatigue pre-crack front to the principal initiation site (coordinate y_3) and fracture toughness.

value of fracture toughness increases with the distance from the fatigue pre-crack to the principal initiation site.

This study offers a semi-quantitative approach to cleavage initiation type and location as a function of testing temperature in a A508 steel.

Acknowledgements

EdF Renardières is acknowledged for providing the specimens. M.M. is grateful for financial support by an Erasmus grant. The work of A.R. is partly funded by a TMR grant (contract No FIS-CT96-5001) provided by DG XII-DEMA.

References

[1] A.H. Cottrell, Trans. Met. Soc. AIME 212 (1) (1958).
[2] E. Smith, Int. J. Fract. Mech. 4 (2) (1968).
[3] G.T. Hahn, Met. Trans. 15A (1984) 947.
[4] N.J. Petch, Acta Metall. 34 (7) (1986) 1387.
[5] J.P. Naylor, Met. Trans. 10A (1979) 861.
[6] P. Brozzo, G. Buzzichelli, A. Mascanzoni, M. Mirabile, Met. Sci. 11 (1977) 123.
[7] S. Matsuda, T. Inoue, H. Mimura, Y. Okamura, Trans. ISIJ 12 (1972) 325.
[8] T. Saario, K. Wallin, K. Törrönen, J. Eng. Mat. Techn. 106 (1984) 173.
[9] J.H. Tweed, J.F. Knott, Met. Sci. 17 (1983) 45.
[10] J.H. Tweed, J.F. Knott, Acta Metall. 35 (7) (1987) 1401.
[11] D.E. McRobie, J.F. Knott, Mat. Sci. Techn. 1 (1985) 357.
[12] A.R. Rosenfield, D.K. Shetty, A.J. Skidmore, Met. Trans. 14A (1983) 1934.
[13] P. Bowen, J.F. Knott, Met. Sci. 18 (1984) 225.
[14] P. Bowen, J.F. Knott, Int. J. Fracture 28 (1985) 103.
[15] M.T. Miglin, C.S. Wade, W.A. Van Der Sluys, in: J.P. Gudas, J.A. Joyce, E.M. Hacket (Eds.), Fracture Mechanics: Twenty-First Symposium, American Society for Testing and Materials, ASTM 1074, Philadelphia, 1990, p. 238.
[16] G.P. Gibson, M. Capel, S.G. Druce, ESIS/EGF Publ. 9 (1991) 587.
[17] J. Heerens, D.T. Read, A. Cornec, K.-H. Schwalbe, ESIS/EGF Publ. 9 (1991) 659.
[18] A. Brückner-Foit, W. Ehl, D. Munz, B. Trolldenier, Fat. Fract. Eng. Mat. Struct. 13 (1990) 185.
[19] T.J. Baker, F.P.L. Kavishe, J. Wilson, Mat. Sci. Techn. 2 (1986) 576.
[20] St. Renevey, Approches globale et locale de la rupture dans le domaine de transition fragile-ductile d'un acier faiblement allié, Ph.D. Thesis, Université Paris XI, Orsay, France, 1997.
[21] K. Ono, M. Yamamoto, Mat. Sci. Eng. 47 (1981) 247.
[22] R.B. Clough, H.N.G. Wadley, Met. Trans. 13A (1982) 1965.
[23] D. Brooksbank, K.W. Andrews, JISI 206 (1968) 595.
[24] I. Nedbal, J. Siegl, J. Kunz, Ductile initiation of cleavage in Charpy V-notch specimens of bainitic steel A508 Cl.3, Research Report V-KMAT-440/97, 42 p., CVUT-FJFI-KMAT, Prague, 1997.